Calibration of the Intensity-Related Distance Error of the PMD TOF-Camera

Marvin Lindner and Andreas Kolb

Computer Graphics Group
Institute for Vision and Graphics
University of Siegen, Germany

ABSTRACT

A growing number of modern applications such as position determination, online object recognition and collision prevention depend on accurate scene analysis. A low-cost and fast alternative to standard techniques like laser scanners or stereo vision is the distance measurement with modulated, coherent infrared light based on the Photo Mixing Device (PMD) technique.

This paper describes an enhanced calibration approach for PMD-based distance sensors, for which highly accurate calibration techniques have not been widely investigated yet. Compared to other known methods, our approach incorporates additional deviation errors related with the active illumination incident to the sensor pixels. The resulting calibration yields significantly more precise distance information. Furthermore, we present a simple to use, vision-based approach for the acquisition of the reference data required by any distance calibration scheme, yielding a light-weighted, on-site calibration system with little expenditure in terms of equipment.

Keywords: Photo Mixing Device, PMD, Calibration, Intensity, TOF

1. INTRODUCTION

The determination of an object's distance relative to an observer (sensor) is a common field of research in Computer Vision and Image Analysis. During the last centuries, techniques have been developed whose basic principles are still widely used in modern systems, such as laser triangulation, stereo vision and structure from motion.[1–3]

Nevertheless, there is no low-cost, off-the-shelf system available, which provides full-range, high resolution distance information in real-time even for static scenes. Laser scanning techniques, which merely sample a scene row by row with a single laser device are rather time-consuming and impracticable for dynamic scenes. Stereo vision systems on the other hand are computationally very complex due to the search of corresponding points. Furthermore, they suffer from inaccuracy caused by mismatching correspondences in homogeneous object regions.

The Photo Mixing Device (PMD) technology is a rather new and promising approach developed during the last years. Here, the distance is determined by time-of-flight approach using modulated, incoherent light. The observed scene is illuminated by infrared light which is reflected by visible objects and gathered in an array of solid-state image sensors based on CMOS technology.[4–6]

Current calibration approaches either use very simple approaches to cope the problem of depth calibration, e.g. assuming a linear mapping,[7] or model the non-linearity incorporated by the systematic distance deviation[8] combined with the dependency from the integration-time.[9]

The contribution of this paper is an enhanced calibration model. In addition to the above mentioned approaches, the significant distance deviation for PMD cameras related to the amount of incident active light, e.g. due to different object reflectivity, is taken into account (see Fig. 1). Moreover, we present a simple to use vision-based approach to acquire the reference data w.r.t. distance and incident light, using an additional 2D camera.

A short overview of the PMD's functionality and known PMD-calibration techniques is given in Sec. 2 and Sec. 3. The design of our calibration model is described in Sec. 4. Finally, the results are discussed in Sec. 5 which leads to a short conclusion of the presented work in Sec. 6.

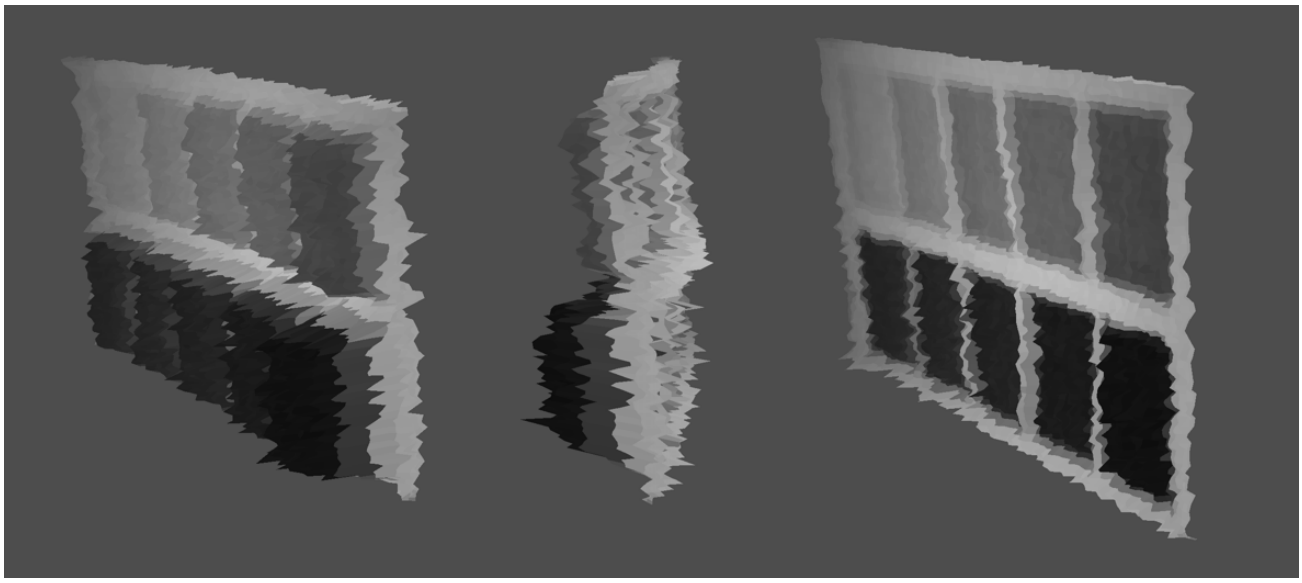

Figure 1. Distance deviation due to varying object reflectivity, i.e. active light incident to the sensor; front and side view (left), after a distance / intensity calibration (right).

2. Photo Mixing Device (PMD)

By sampling and correlating the incoming optical signal with the reference signal of the modulated, incoherent illumination directly on a pixel, the PMD is able to determine the signal's phase shift and thus the distance information by a time-of-flight approach.[4–6]

Given a reference signal $g(t)$ and the optical signal $s(t)$ incident to a PMD pixel, the pixel samples the correlation function $c(\tau)$ for a given internal phase delay τ:

$$c(\tau) = (s \otimes g)(\tau) = \lim_{T\to\infty} \int_{-T/2}^{T/2} s(t) \cdot g(t+\tau)\, dt.$$

For a sinusoidal signal $g(t) = \cos(\omega t)$ and the optical response signal $s(t) = k + a\cos(\omega t + \phi)$ basic trigonometric calculus yields (see Lange[5] for more details):

$$c(\tau) = h + \tfrac{a}{2}\cos(\omega\tau + \phi)$$

where ω is the modulation frequency, a and h is the amplitude and the offset of the correlation function, respectively, and ϕ is the phase shift relating to the object distance. The modulation frequency defines the distance unambiguousness of the distance sensing. The demodulation of the correlation function is done using several samples of $c(\tau)$ obtained by four sequential PMD raw images $A_i = c(\tau_i)$ using internal phase delays $\tau_i = i \cdot \frac{\pi}{2},\ i = 0, \ldots, 3$:

$$\begin{aligned} \phi &= \arctan\left(\frac{A_3 - A_1}{A_0 - A_2}\right) \\ a &= \frac{\sqrt{(A_3 - A_1)^2 + (A_0 - A_2)^2}}{2} \\ h &= \frac{A_0 + A_1 + A_2 + A_3}{4}. \end{aligned} \tag{1}$$

Knowing ϕ, the object distance m measured in a single pixel is given by $m = c\phi/4\pi\omega$, where c is the speed of light. A measure of the distance quality is represented by the amplitude a of the correlation function. The accuracy of the measured distance information relies on the amount of incident active light, which is influenced e.g. by the

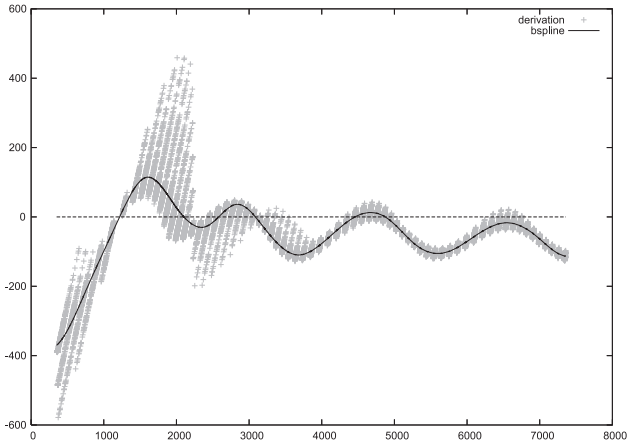

Figure 2. Systematic deviation error between 0 - 7.5 m. Due to an modified illumination unit, an over-saturation occurs in the closeup range up to 3 m (from[8]).

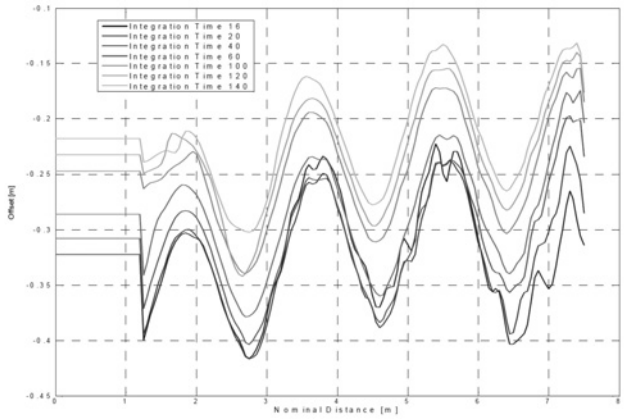

Figure 3. Exemplary Look Up Table (LUT) for different integration times published by Kahlman et al..[9]

IR-reflectivity and the object orientation. Another problem in this context concerns the relatively large size of the solid angle corresponding to a PMD pixel. The demodulation generally assumes distance homogeneity inside a solid angle. In reality different distances inside a solid angle occur and lead to superimposed reflected light reducing its amplitude and distorting the phase shift ϕ. Finally, the pixel intensity is given by the offset h of the correlation function, which stands for the amount of reflected light.

The manufacturing of a PMD chip is based on standard CMOS-processes which allows a very economic production of a device which is, due to an automatic suppression of background light, suitable for indoor as well as outdoor scenes. Current devices provide a resolution of 48×64 or 160×120 px at 20 Hz, which is of high-resolution in the context of dynamic depth sensing but still of low-resolution in terms of image processing. A common modulation frequency is 20 MHz, resulting in an unambiguous distance range of 7.5 m. An approach to overcome the limited resolution of the PMD camera is its combination with a 2D-sensor.[10]

3. RELATED WORK

There are three major causes for distance errors for PMD-based depth sensors. First, there is always some discrepancy between the theoretical considered sinusoidal signal and the actual signal form resulting in the *systematic distance error*. The other error sources are based on the variation of the *integration-time* and the amount of *incident light* (see Fig. 1).

In Lindner and Kolb[8] we presented an approach which essentially uses uniform B-splines to model the systematic distance deviation between measured distance information of a given PMD camera and a known reference plane (see Fig. 2). The model itself is a two step approach, which uses a uniform B-spline as a global correction function and a linear function for a per pixel pre- and post-adjustment, coping with the pixel's individual behavior. The global B-spline is derived using a least-squares fit to all distance samples.

By separating the calibration into two steps, a comparatively high accurate distance calibration can be archived, by storing a small number of calibration parameter at the same time. A set of calibration parameter consists of about 10 - 15 control points for the global B-spline and additional two parameter for each pixel to store the linear pre-adjustment.

A similar calibration approach has been introduced by Kahlmann et al..[9] Here, a lookup table is used to store the distance deviation between measured and real distance information of a plane wall for different integration times (see Fig. 3). Given an integration time and a measured distance information, the deviation is determined by linear interpolation between two consecutive table entries.

However, the distance deviation is grabbed using a single PMD-pixel only. A pixel-wise pre-adjustment is done by a so called *Fixed Pattern Noise* matrix, containing an individual, constant offset for every pixel. The

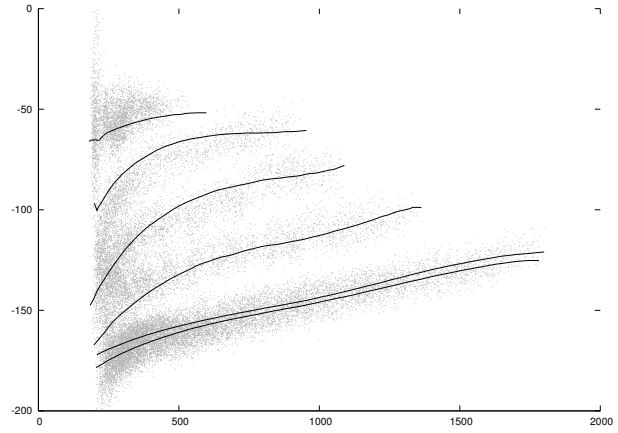

Figure 4. Distance deviation for different reference distances in the range 90-190 cm depending on the incident light (gray) and deviation data evaluating the depth-intensity calibration for the given input parameter (black)

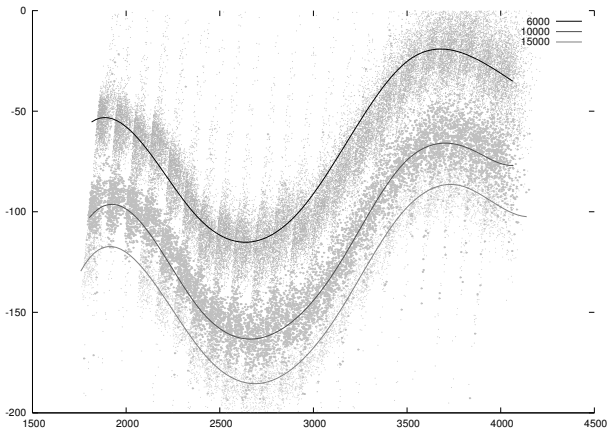

Figure 5. Distance deviation due to different shutter times. Longer shutter times cause the measured distances to drift towards the camera. The distinctive curve progression remains maintained.

constant per-pixel offset is determined by means of comparison between the measured distances and the reference distance, calculated out of the camera coordinates using an external localization system.

Both approaches use reference distance data for the distance calibration which has been acquired on high accuracy distance measurement track lines.

4. PMD CALIBRATION METHOD

In the Section we describe our novel calibration method, which incorporates all three error sources, namely the systematic error and the error based on varying incident light and on integration time. First, Sec. 4.1 describes our vision-based approach for acquiring 3D reference data. The calibration model and the adjustment made for integration-based error is explained in Sec. 4.2 and Sec. 4.3, respectively.

4.1 Vision-Based Data Acquisition

One of our goals in the context of depth calibration is the implementation of a vision-based approach, which can be used without any special equipment, such as track lines.

The basic idea is to use extrinsic parameter calculations as provided by standard libraries like Intel's computer vision library OpenCV.[11] These extrinsic parameters are used for pose estimation of the tracked panel, yielding the required distance references.

However, due to the low resolution of the PMD camera, the extrinsic parameters estimation is either inaccurate or time-consuming. The vision-based data acquisition therefore uses a simple binocular combination of a PMD- and a 2D RGB-camera with fixed relative position and maximal overlap for the field-of-views (see Fig. 6). The acquisition process now uses the RGB-camera for a robust estimation of extrinsic parameters w.r.t. the tracked panel, which then can be transformed into the coordinate system of the PMD-camera. The second step requires an initial simultaneous 2D calibration of both cameras.

The data acquisition can be summarized as follows:

1. 2D calibration for PMD- and 2D camera using OpenCV, yielding extrinsic transformations $T_{\mathrm{PMD}\rightarrow\mathrm{World}}$ and $T_{\mathrm{RBG}\rightarrow\mathrm{World}}$
2. Transformation between RGB- and PMD-camera: $T_{\mathrm{RGB}\rightarrow\mathrm{PMD}} = T^{-1}_{\mathrm{PMD}\rightarrow\mathrm{World}} \cdot T_{\mathrm{RGB}\rightarrow\mathrm{World}}$
3. 3D data acquisition:

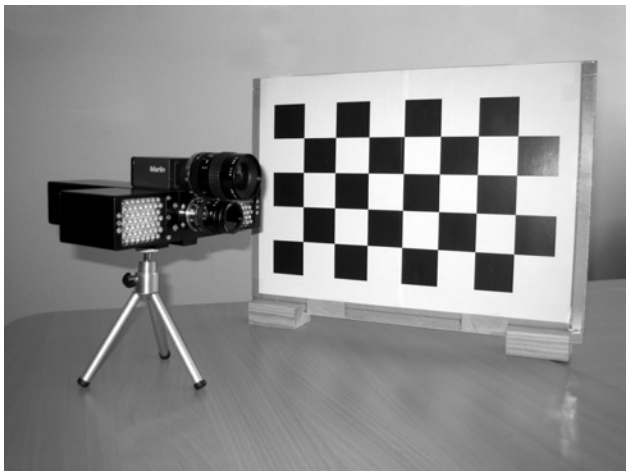

Figure 6. 2D/3D camera setup consisting of a 19k PMD and a high-resolution CCD-camera. On the right site an exemplary calibration panel can be seen.

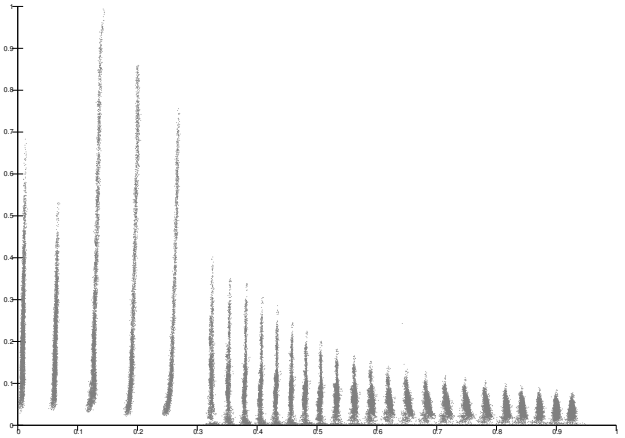

Figure 7. Sample points in respect of measured distance (x-axis) and intensity (y-axis) with integration time $T = 6000\mu s$. In the near range, several samples have been suppressed due to over-saturation.

3.1. simultaneous acquisition for an RGB- and a PMD (distance) image

3.2. compute extrinsic parameters to the 2D calibration panel using the extrinsic parameter of the RGB-camera

3.3. transform panel plane equation from RGB- to PMD coordinate system using $T_{\mathrm{RGB}\rightarrow\mathrm{PMD}}$

3.4. compute reference distances for each pixel by a simple ray-plane intersection

Since we incorporate also the distance error due to varying incident light, we also need different amounts of incident light for all pixels. Therefore, we use a simple several panels with different IR reflectivity, allowing to measure distances and various gray-levels.

4.2 Intensity-Related Distance-Error

Both approaches mentioned in Sec. 3 only model the systematic distance error. Kahlmann et al.[9] additionally incorporate the integration time into their calibration model.

Indeed, adjusting the systematic error results in increased accuracy for the distance measurement. However, it can be clearly observed, that objects with lower reflectivity have a significant drift towards the camera, i.e. the distance decreases with decreasing reflectivity (see Fig. 1). This phenomenon is mainly observable in the near range, but is also still recognizable in regions further away from the sensor (see Fig. 4).

As the reflectivity correlates with the active light incident to each sensor pixel, we can use the h-parameter to detect this effect, in order to set up an appropriate calibration model (see Eq. (2)).

Fig. 4 shows the distance deviation for four different panel distances w.r.t. the measured pixel intensity. The plot clearly exhibits a non-trivial dependency of the distance deviation from the incident light, which also significantly varies between different reference distances. This clearly shows, that the two error dimensions, i.e. systematic distance error and error due to incident light, are not independent, thus both effects can not be handled separately.

Our distance calibration model uses a bi-variate correction function for the distance adjustments, where the two parameters are the measured distance $m = c\phi/4\pi\omega$ and the intensity h (see Eq. (2)), where c is the speed of light. We use a *full-range* approximation approach similar to our previous approach,[8] i.e. we take all pixels into account. Like before, we use a B-Spline to model the distance deviation dependent from these two parameters:

$$P(m,h) = \sum_{i=1}^{p}\sum_{j=1}^{q} N_i^3(m)\cdot N_j^3(h)\cdot c_{ij}, \tag{2}$$

where N_i^3 are the uniform cubic B-spline basis functions over a set of control points with size $p \cdot q$.

Assuming a set of input data $\{(m_k, h_k, d_k)\}_{k \in \mathcal{K}}$ consisting of a set $\mathcal{K}$ of triples of measured distances m_k, incident light h_k and reference distance (ground truth) d_k for a fixed integration time T, we get a set of constraints for the unknown B-spline coefficients c_{ij} from Eq. (2):

$$\sum_{i=1}^{p} \sum_{j=1}^{q} N_i^3(m_k) \cdot N_j^3(h_k) \cdot c_{ij} = m_k - d_k, \; k \in \mathcal{K} \tag{3}$$

Rearranging the set of equations in (3) by writing the unknown coefficients c_{ij} as vector $\vec{\mathbf{c}} = (c_{11}, c_{12}, \ldots, c_{1m}, c_{21}, \ldots, c_{nm})^T$, we derive a linear system of equations

$$A \cdot \vec{\mathbf{c}} = \vec{\delta} \tag{4}$$

with $\delta = (m_1 - d_1, \ldots, m_{|\mathcal{K}|} - d_{|\mathcal{K}|})^T$ and

$$A = \left[\; N_i^3(m_k) \cdot N_j^3(h_k) \; \right]_{\substack{(i,j) = (1,1), \ldots, (n,m) \\ k = 1, \ldots, |\mathcal{K}|}} \tag{5}$$

In general, we can not guarantee, that there are enough constraints in all parameter regions of the bi-variate B-spline. Especially for larger distances, we do not have samples for high incident active light, due to the attenuated light intensity (see Fig. 7). Thus, in general, matrix A in Eq. (4) is not of full rank. To avoid numerical instabilities in sparsely sampled parameter regions, we add a smoothing constraint using the Laplace operator:

$$\nabla P(m,h) = \nabla \frac{\partial^2 P}{\partial m^2}(m,h) + \frac{\partial^2 P}{\partial h^2}(m,h) = 0 \tag{6}$$

Applying the derivation rules for B-splines and the fact, that B-splines form a function basis, (6) is equivalent with

$$\begin{aligned} 4 \cdot c_{i,j} - (c_{i-1,j} + c_{i,j-1} + c_{i+1,j} + c_{i,j+1}) = 0, \\ (i,j) = (2,2), \ldots, (n-1, m-1). \end{aligned} \tag{7}$$

Extending matrix A by these smoothing constraints (7), we can guarantee the full rank of the resulting matrix $\tilde{A}$:

$$\tilde{A} \cdot \vec{\mathbf{c}} = \begin{bmatrix} A \\ \lambda L \end{bmatrix} \cdot \vec{\mathbf{c}} = \begin{bmatrix} \vec{\delta} \\ 0 \end{bmatrix}, \tag{8}$$

where L contains the Laplace-constraints and λ controls the amount of smoothing.

With the guaranty of a full rank, the extended linear equation system in Eq. 8 can be now solved using a least square optimization also known as pseudo inverse approach:

$$\vec{\mathbf{c}} = (\tilde{A}^T \tilde{A})^{-1} \tilde{A}^T \cdot \tilde{\delta} \tag{9}$$

With regard to the original calibration model,[8] an asymmetric pixel-wise pre-adjustment is performed using distance informations only. Generally, no reference value for the intensity parameter is known, thus no canonically extension of the pre-adjustment exists for the intensity values.

4.3 Shutter-Time-Related Distance-Error

As mentioned by Kahlman et al.,[9] there exists some dependency between the distance error and the shutter time for PMD-based the TOF-cameras. We observe the same, i.e. with increasing integration time the whole scene shifts towards the camera.

To take the different integration times into account, the calibration model is extended by the successive processing of appropriate input data for several integration times. Given an integration time, the proper set of control points is computed during the distance adjustment using simple linear interpolation of the B-spline control points.

Alternatively, one can also generate a 3D lookup table instead of storing the individual deviation functions.

Ref	Unc.	Distance only			Dist. & Intens.		
[cm]	[mm]	⊘	0%	70%	⊘	0%	70%
90	157.7	19.4	1.0	25.3	3.5	2.8	3.2
110	157.6	28.2	2.1	35.0	3.8	2.3	3.2
130	131.4	21.0	3.0	32.4	6.4	3.1	4.0
170	88.8	28.9	2.1	37.2	9.7	4.2	11.3
210	65.3	13.5			10.0		
250	110.2	17.3			15.2		
300	106.4	15.9			11.3		
350	30.8	21.8			11.8		
400	35.4	26.7			17.3		

Table 1. Distance deviation in [mm] for several reference distances before (Unc.) and after a distance adjustment has been performed. In the near range, both the average of all as well as the distance error for 20 % and 70% black are listed. The systematic error due to the demodulation can be clearly seen in the uncorrected distance data.

5. RESULTS

In order to determine the improvement of the enhanced calibration model compared to the existing models, both methods (distance only and distance in combination with intensity) has been used to adjust the given distance information of the same set of input data.

In the case of pure distance adjustment, the B-spline has been fitted to the white images, which possess the fewest noise interferences. This correction is applied to the complete input data, independent of the actual light incident to a PMD pixel.

During the acquisition step of the calibration input data, the intensity channel of each image has been de-noised by a *black image* taken with the lense of the PMD camera kept shut. This results in a fixed noise pattern caused by the individual intensity characteristics of each pixel. However, test results have shown, that de-noising of the input intensity does not improve the result of the distance adjustment. However, it should be noted, that one has to decide whether to use the black image correction in both steps, i.e. when determining the calibration parameters and applying the distance adjustment, or never. Otherwise the calibration quality will be reduced significantly.

Tab. 1 shows the mean deviation error for both methods w.r.t. different reference distances. Here, we have used 10 and 5 control points for the distance and the intensity component, respectively, and a smoothing factor $\lambda = 1$.

It can be seen, that the original calibration models, which handle distance information only, still adjust the high reflective images correctly, but fail on the images with low reflectivity.

In contrast, the enhanced calibration model, which takes distance and intensity into account, is able to correct all images independent from the incident light (cp. Fig. 1).

6. CONCLUSION

This paper describes an enhanced calibration model, which includes the so far neglected handling of intensity, i.e. incident light, caused by object reflectivity. Observations have shown that distance deviation errors due to different reflectivity properties have significant effects and thus, they are regarded in our novel calibration model. We use a parametric bi-variate B-spline as correction function. Applying our calibration model, a significant reduction of the distance error can be observed. Additionally, we have introduced a simple to use, on-site approach for capturing the reference data required for the estimation of the calibration parameters.

7. ACKNOWLEDGMENTS

This work is partly supported by the German Research Foundation (DFG), KO-2960/5-1. Furthermore we would like to thank PMDTechnologies Germany.

REFERENCES

1. O. Faugeras, *Three-dimensional Computer Vision*, The MIT Press, 1993.
2. R. I. Hartley and A. Zisserman, *Multiple View Geometry in Computer Visio*, Cambridge University Press, ISBN: 0521540518, second ed., 2004.
3. G. K. Henry, *Three Dimensional Vision by Laser Triangulation*. PhD thesis, 1988.
4. H. Kraft, J. Frey, T. Moeller, M. Albrecht, M. Grothof, B. Schink, H. Hess, and B. Buxbaum, "3D-camera of high 3D-frame rate, depth-resolution and background light elimination based on improved PMD (photonic mixer device)-technologies," in *OPTO*, 2004.
5. R. Lange, *3D Time-Of-Flight Distance Measurement with Custom Solid-State Image Sensors in CMOS/CCD-Technology*. PhD thesis, University of Siegen, 2000.
6. Z. Xu, R. Schwarte, H. Heinol, B. Buxbaum, and T. Ringbeck, "Smart pixel – photonic mixer device (PMD)," in *Proc. Int. Conf. on Mechatron. & Machine Vision*, pp. 259–264, 1998.
7. K.-D. Kuhnert and M. Stommel, "Fusion of stereo-camera and pmd-camera data for real-time suited precise 3D environment reconstruction," in *Proc. Int. Conf. on Intelligent Robots and Systems*, pp. 4780–4785, 2006.
8. M. Lindner and A. Kolb, "Lateral and depth calibration of PMD-distance sensors," in *Int. Symp. on Visual Computing (ISVC)*, **2**, pp. 524–533, Springer, 2006.
9. T. Kahlmann, F. Remondino, and H. Ingensand, "Calibration for increased accuracy of the range imaging camera SwissRanger$^{\text{TM}}$," in *Image Engineering and Vision Metrology (IEVM)*, 2006.
10. T. Prasad, K. Hartmann, W. Weihs, S. Ghobadi, and A. Sluiter, "First steps in enhancing 3D vision technique using 2D/3D sensors," in *11th Computer Vision Winter Workshop 2006*, V. Chum, O.Franc, ed., pp. 82–86, 2006.
11. Intel Inc., "Open source computer vision library (OpenCV)." `www.intel.com/technology/computing/opencv/`.